APPLIED PHYSICS LETTERS VOLUME 82, NUMBER 10 10 MARCH 2003

The role of hole leakage in 1300-nm InGaAsN quantum-well lasers

Nelson Tansu[a] and Luke J. Mawst
Reed Center for Photonics, Department of Electrical Computer Engineering, University of Wisconsin-Madison, 1415 Engineering Drive, Madison, Wisconsin 53706-1691

(Received 16 August 2002; accepted 10 January 2003)

We calculate the thermionic escape times of electrons and holes in InGaAsN and InGaAs quantum wells using the most recent input data. The short thermionic escape time of holes from the InGaAsN quantum well indicates that hole leakage may be a significant factor in the poorer temperature characteristics of InGaAsN quantum-well lasers compared to those of InGaAs devices. We suggest a structure that results in an increased escape time, which will allow the reduction of hole leakage in these devices. © *2003 American Institute of Physics.* [DOI: 10.1063/1.1558218]

The poor temperature characteristics of 1.3-μm, InP-based semiconductor lasers have led to enormous efforts in exploring InGaAsN quantum-well (QW) lasers,[1–8] as an alternative to realize high-performance QW lasers for high-temperature operation. Early high threshold-current-density (J_{th}) 1300-nm InGaAsN single-quantum-well (SQW) lasers exhibit anomalously high T_0 ($1/T_0 = (1/J_{th}) dJ_{th}/dT$) values, due to the large monomolecular recombination.[9,10] Unfortunately, the T_0 values of the high-performance 1300-nm InGaAsN SQW lasers are only 70–110 K,[1–5,8] which is low compared to those of the 1200-nm InGaAs SQW lasers ($T_0 = 200$ K).[1] The underlying cause for the relatively low T_0 values for InGaAsN lasers has not been conclusively determined. Recent analysis without taking account of carrier leakage processes, has attributed the low T_0 values to the existence of Auger recombination in the InGaAsN QW.[10] In our earlier work,[9] the reduced T_0 and T_1 ($1/T_1 = -(1/\eta_d) d\eta_d/dT$, η_d = external differential quantum efficiency) values of the 1300-nm InGaAsN QW lasers, compared to 1190-nm InGaAs QW lasers, has been linked to an increase in the carrier/current leakage processes. Despite the deeper QW structure in the InGaAsN QW lasers, the experimentally measured current injection efficiency (η_{inj}) of 1300-nm InGaAsN QW reduces more rapidly with temperature compared to that of the 1200-nm InGaAs QW lasers.[9] As N is added into the QW to push the emission wavelength longer, experiments have indicated the η_{inj} of InGaAsN QW lasers decreases as a function of increasing N content.[1,8] The reduction in η_{inj} can result from active-layer carrier leakage. Here, we identify a carrier-leakage process in InGaAsN QW lasers[9] as heavy-hole (hh) leakage due to poor active-layer hole confinement.

The thermionic carrier lifetime (τ_e) in QW lasers is an important factor in determining the η_{inj} of a laser.[11,12] A large thermionic lifetime of the carriers in the QW indicates a minimal escape rate of the carriers from the QW to the separate confinement heterostructure (SCH).[11,12] Minimal thermionic carrier escape rate out of the QW will lead to an increase in η_{inj} and a reduction in the temperature sensitivity of η_{inj}.[11,12] The conventional method to express the thermionic lifetime is based on the model by Schneider *et al.*,[13] which utilizes the bulk [three-dimensional (3-D)] density of states (DOS) and a simple parabolic band model. However, this model[13] has been shown to be insufficient to explain experiments,[14] and has a tendency to significantly overestimate the hole lifetime and to underestimate the electron lifetime.[14] The thermionic lifetime model that we employ in this study is based on the model proposed by Irikawa *et al.*,[14] that has been applied to the study of 1500-nm InGa(Al)As/InP QW lasers.

The thermionic current leakage, from the edge of the QW to *one side* of the SCH, J_{ee_i}, is related to the thermionic emission carrier lifetime to *one side* of the SCH τ_{ee_i}, as follows: $J_{ee_i} = NqL_zN_{QW}/\tau_{ee_i}$, in which i, N, q, L_z, and N_{QW}, represent the type of carriers (electrons or holes), the number of QWs, the electron charge, the QW thickness, and the carrier density in QW, respectively. It is important to note that the thermionic leakage current here is not the same as the total current leakage in QW laser devices, as the leaked carriers into the SCH region have the probability of being recaptured back and recombine in the QW.[11,12,14] The relationships of the total threshold current density and the current injection efficiency with the thermionic carrier lifetime are more complex, and are interrelated by the total recombination lifetime in the QW and barrier regions and carrier capture time into the QW.[11,12,14] The leakage current J_{ee_i} has been described in Refs. 13 and 14 with the standard thermionic emission theory, as follows:

$$J_{ee_i} = \frac{4\pi q (k_B T)^2}{h^3} m_i^* \exp\left(-\frac{E_{bi} - F_i}{k_B T}\right), \tag{1}$$

where m_i^*, E_{bi}, and F_i are the effective masses of the electrons or holes in the QW, the effective barriers and the quasi-Fermi levels for the electrons or holes in QW, respectively. The constants k_B and h represent the Boltzmann and Planck constants, respectively. The carrier density in the QW is calculated by taking into consideration the two-dimensional (2-D) DOS of the strained QW, strain effects in band gap of the QW, and the Fermi–Dirac statistics.[15] The thermionic escape lifetime (τ_{ee_i}) can be extracted by relating the thermionic leakage current (J_{ee_i}) and the carrier density in the QW (N_{QW}), with consideration of the structure. The total current leakage from the SQW to *both sides* of the SCH,

[a]Email: tansu@cae.wisc.edu

 © 2003 American Institute of Physics
Downloaded 20 Jul 2011 to 128.180.137.141. Redistribution subject to AIP license or copyright; see http://apl.aip.org/about/rights_and_permissions

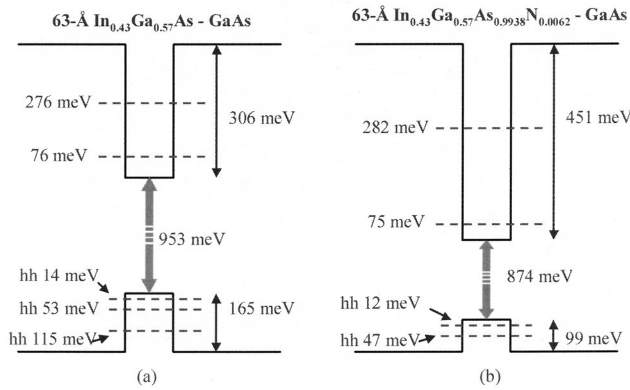

FIG. 1. Band line-up for conduction and valence bands of (a) 1190-nm $In_{0.43}Ga_{0.57}As$ QW and (b) 1295-nm $In_{0.43}Ga_{0.57}As_{0.9938}N_{0.0062}$ QW lasers, with GaAs barriers.

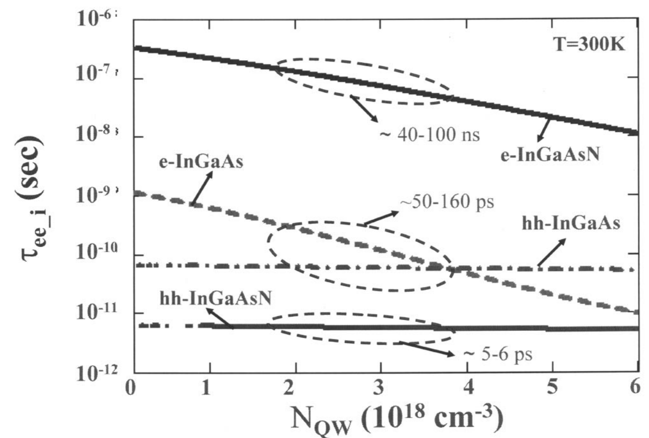

FIG. 2. The electron- and hole-thermionic escape lifetimes of 1190-nm $In_{0.43}Ga_{0.57}As$ QW and 1295-nm $In_{0.43}Ga_{0.57}As_{0.9938}N_{0.0062}$ QW lasers with GaAs barriers, at a temperature of 300 K, as functions of carrier density.

contributed by carrier i (electrons or holes), is $J_{e_i} = J_{ee_i_right} + J_{ee_i_left}$. The *total* thermionic escape lifetime of carrier i (τ_{e_i}) can be expressed as $1/\tau_{e_i} = 1/\tau_{ee_i_right} + 1/\tau_{ee_i_left}$. For the case of symmetrical barriers ($J_{ee_i_right} = J_{ee_i_left}$), the expression $1/\tau_{e_i} = 2/\tau_{ee_i}$ will be obtained.

In this study, the τ_{ee_i} values are analyzed for the case of the 1190-nm emitting InGaAs QW and 1300-nm emitting InGaAsN QW lasers. These 1190–1300-nm InGaAs(N) QW lasers, shown schematically in Fig. 1, are similar to lasers that have been published previously,[1,2] in which a very high In-content (~40%) and minimum N-content (~0.5%) InGaAs(N) QW are utilized to achieve high-performance $\lambda = 1190$–1300-nm emitting lasers with GaAs as the *direct* barrier to the QW. Large-band-gap $Al_{0.74}Ga_{0.26}As$ layers are utilized as the *n*- and *p*-cladding layers, to ensure minimal carrier leakage from SCH region to cladding layers. The existence of the small N content (~0.5%–2%) in the InGaAsN QW affects mainly the conduction band, which allows for the approximation of many of the material parameters of the $In_xGa_{1-x}As_{1-y}N_y$ QW with those of the $In_xGa_{1-x}As$ QW.[16] The compilation of the parameters used here follows the treatment in Refs. 16 and 17 for the effective masses of the electrons, band-gap energy, and conduction (ΔE_c)- and valence (ΔE_v)-band offsets.

We determine the approximate band-offset values by fitting the theory with the *measured* values from the experiments. The conduction-band-offset ratio ($Q_c = \Delta E_c / \Delta E_g$) for highly strained (In>20%) InGaAs–GaAs materials has been predicted to be in the range of 60% to 65%.[15,18–20] For the case of the InGaAsN QW, *experimental* studies,[7,17] show that Q_c is as high as 77%–80% for the case of $In_{0.38}Ga_{0.62}As_{0.985}N_{0.015}$. Additional recent work[21] has also demonstrated *experimentally* the reduction in the valence-band offset (ΔE_v) in InGaAsN QW as a result of N incorporation into the InGaAs QW. We found very good agreement in emission wavelength and QW composition between theory and experiment, with Q_c values of 65% and 82% for 63-Å $In_{0.43}Ga_{0.57}As$ QW, and the 63-Å $In_{0.43}Ga_{0.57}As_{0.9938}N_{0.0062}$ QW, respectively. The compositions, the QW thickness, and the emission wavelengths of both the 60-Å $In_{0.4}Ga_{0.6}As$ QW and 60-Å $In_{0.4}Ga_{0.6}As_{0.995}N_{0.005}$ QW are measured experimentally.[1,22] The m_e^* for InGaAs QW and InGaAsN QW here are calculated as $0.047m_o$ and $0.069m_o$, respectively, with m_o as mass of electron. The m_{hh}^* for both InGaAs and InGaAsN QW utilized in calculation is $0.457m_o$. Due to the large strain of the InGaAs and InGaAsN QW, the hole band-structure consists of only hh subbands in the 2-D states, with light-hole states having bulk-like (3-D) properties.

By utilizing the parameters listed in Refs. 14–20 and in Fig. 1, the τ_{ee_i} can be calculated for electrons and holes for both InGaAs and InGaAsN QWs, as shown in Fig. 2. For the case of an InGaAs QW, the τ_{ee} (~50–160 ps) of electrons is comparable to that (~55–60 ps) of heavy holes, for typical threshold carrier density of interest ($N_{QW} \sim 1.5$–4×10^{18} cm^{-3}). In the case of an InGaAsN QW, the τ_{ee} of the heavy hole is significantly smaller than τ_{ee} of the electron. The electrons are very well confined in InGaAsN QW, as indicated by the large τ_{ee} (~40–100 ns) of the electron for typical threshold conditions. This large τ_{ee} of electrons in InGaAsN QW is expected, owing to its large conduction-band offset ($\Delta E_c \sim 450$ meV). On the other hand, the heavy hole is very poorly confined due to the large disparity of the ΔE_c and ΔE_v. The small valence-band offset ($\Delta E_c \sim 99$ meV) in InGaAsN QW results in picosecond-range τ_{ee} of approximately 5–6 ps, for typical threshold conditions. Due to the significantly smaller τ_{ee} of the hole in InGaAsN QW, the hh leakage is the dominant leakage mechanism for the InGaAsN QW. Severe thermionic carrier leakage leads to a reduction in the η_{inj} at threshold,[11,12] distinct from the above-threshold η_{inj},[23] and will in turn lead to an increase in the J_{th} of the QW laser.

The τ_{ee_i} for the InGaAs and InGaAsN QWs are shown in Figs. 3(a) and 3(b). At elevated temperature ($T = 360$ K), τ_{ee} of the heavy hole reduces to only 3 ps. In the case of the InGaAs QW, the lowest τ_{ee} is approximately 21 ps at an elevated temperature of 360 K. The severe hh leakage at elevated temperature for InGaAsN QW lasers, serves as one of the contributing factors that leads to the highly temperature-sensitive ($T_0 \sim 70$–90 K) threshold current of high-performance, 1300-nm InGaAsN QW lasers. Though the hole-leakage processes play a vital role in InGaAsN QW lasers at high temperature, Auger recombination and other

Downloaded 20 Jul 2011 to 128.180.137.141. Redistribution subject to AIP license or copyright; see http://apl.aip.org/about/rights_and_permissions

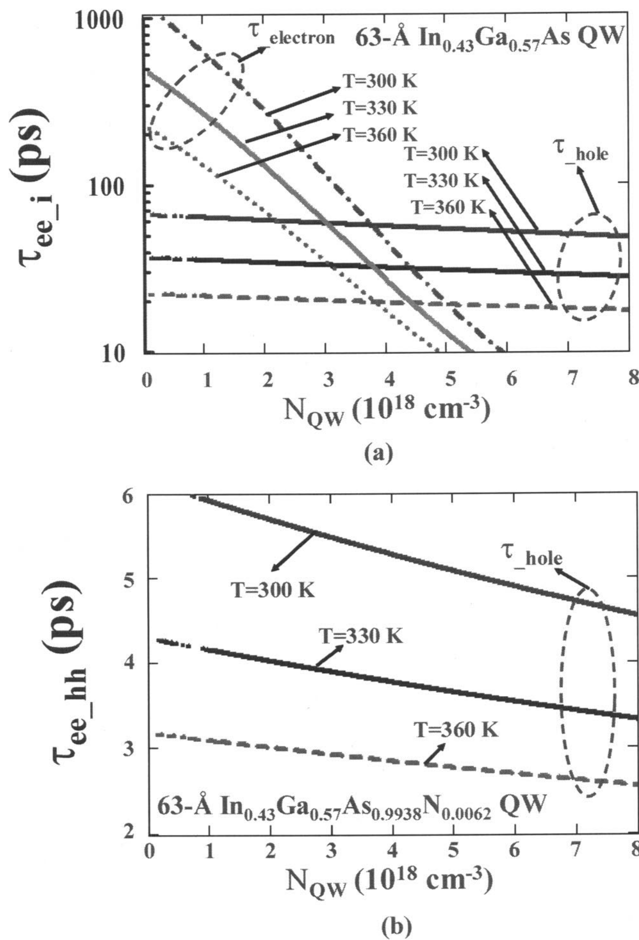

FIG. 3. The electron- and hole-thermionic escape lifetimes of the (a) 1190-nm InGaAs QW and (b) the 1295-nm InGaAsN QW lasers with GaAs barriers, as functions of carrier density and temperature.

processes cannot be ruled out as contributing factors.

To achieve suppression of hole leakage from the InGaAsN SQW, larger-band-gap materials of tensile GaAsP or InGaAsP can also be utilized as the direct barrier or SCH regions. As shown in Fig. 4, the τ_{ee} of holes in an InGaAsN QW are calculated for structures with various barrier regions. By utilizing the 1.77-eV InGaAsP lattice-matched barriers, with the assumption of a band-offset ratio ($\Delta E_c:\Delta E_v$) of 82:18, the thermionic escape rate ($1/\tau_{ee_h}$) of the heavy-hole in InGaAsN QW is reduced significantly by approximately 10–12 times, in comparison with that of the InGaAsN–GaAs case. In fact, the τ_{ee_h} ($\sim$25 ps, $N_{QW}\sim 3\times 10^{18}$ cm^{-3}, $T=360$ K) of the heavy-hole for an InGaAsN QW with 1.77-eV barriers at elevated temperature, is comparable with the lowest τ_{ee} of carriers in an InGaAs QW for typical threshold conditions at the same temperature. The utilization of an InGaAsN multiple QW with GaAs barriers, is also expected to improve the high-temperature laser performance. The utilization of multiple QW lasers will result in a lower thermionic hole escape rate ($1/\tau_{ee_h}$), as the $1/\tau_{ee}$ is inversely proportional to the number of QWs (N).

The hole-leakage process is identified as the main mechanism in the leakage process in 63-Å $In_{0.43}Ga_{0.57}As_{0.9938}N_{0.0062}$ SQW lasers with GaAs barriers. Reduction in the hole leakage, by utilizing large-band-gap barriers in a SQW, should allow the realization of high-

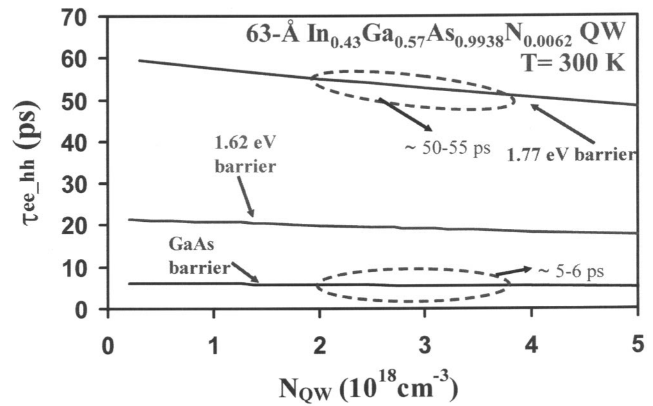

FIG. 4. The electron- and hole-thermionic escape lifetimes of the 1295-nm InGaAsN QW lasers with various barriers, at temperature of 300 K, as functions of carrier density.

lasing-performance and high-temperature-operation 1300-nm InGaAsN SQW lasers. Due to the complexity in determining the parameters for InGaAsN materials, it is not the intent of this letter to provide the most accurate values of the thermionic carrier escape time from InGaAsN QW. Rather it is to point out the significance of the thermionic carrier escape processes in 1300-nm InGaAsN QW lasers, which have been neglected in previous analysis under the assumption of strong electron confinement.

[1] N. Tansu, and L. J. Mawst, IEEE Photonics Technol. Lett. **14**, 444 (2002).
[2] N. Tansu, N. J. Kirsch, and L. J. Mawst, Appl. Phys. Lett. **81**, 2523 (2002).
[3] F. Hohnsdorf, J. Koch, S. Leu, W. Stolz, B. Borchert, and M. Druminski, Electron. Lett. **35**, 571 (1999).
[4] C. S. Peng, T. Jouhti, P. Laukkanen, E.-M. Pavelescu, J. Konttinen, W. Li, and M. Pessa, IEEE Photonics Technol. Lett. **14**, 275 (2002).
[5] D. A. Livshits, A. Yu. Egorov, and H. Riechert, Electron. Lett. **36**, 1381 (2000).
[6] W. Ha, V. Gambin, M. Wistey, S. Bank, S. Kim, J. S. Harris, Jr., IEEE Photonics Technol. Lett. **14**, 591 (2002).
[7] M. Kondow, T. Kitatani, S. Nakatsuka, M. C. Larson, K. Nakahara, Y. Yazawa, M. Okai, and K. Uomi, IEEE J. Sel. Top. Quantum Electron. **3**, 719 (1997).
[8] J. Wei, F. Xia, C. Li, and S. R. Forrest, IEEE Photonics Technol. Lett. **14**, 597 (2002).
[9] N. Tansu, and L. J. Mawst, IEEE Photonics Technol. Lett. **14**, 1052 (2002).
[10] R. Fehse, S. Tomic, A. R. Adams, S. J. Sweeney, E. P. O'Reilly, A. and H. Riechert, IEEE J. Sel. Top. Quantum electron. **8**, 801 (20020.
[11] R. Nagarajan and J. E. Bowers, IEEE J. Quantum Electron. **29**, 1601 (1993).
[12] N. Tansu and L. J. Mawst (unpublished).
[13] H. Schneider and K. V. Klitzing, Phys. Rev. B **38**, 6160 (1988).
[14] M. Irikawa, T. Ishikawa, T. Fukushima, H. Shimizu, A. Kasukawa, and K. Iga, Jpn. J. Appl. Phys. **39**, 1730 (2000).
[15] S. L. Chuang, *Physics of Optoelectronic Devices* (Wiley, New York, 1995).
[16] W. W. Chow, E. D. Jones, N. A. Modine, A. A. Allerman, and S. R. Kurtz, Appl. Phys. Lett. **75**, 2891 (1999).
[17] M. Hetterich, M. D. Dawson, A. Yu. Egorov, D. Bernklau, and H. Riechert, Appl. Phys. Lett. **76**, 1030 (2000).
[18] B. Jogai, Appl. Phys. Lett. **59**, 1329 (1991).
[19] J. J. Coleman, in *Quantum Well Lasers*, edited by P. S. Zory, (Academic, New York, 1993), Chap. 8.
[20] S. Niki, C. L. Lin, W. S. C. Chang, and H. H. Wieder, Appl. Phys. Lett. **55**, 1339 (1989).
[21] J. B. Heroux, C. Yang, and W. I. Wang, J. Appl. Phys. **92**, 4361 (2002).
[22] N. Tansu, Y. L. Chang, T. Takeuchi, D. P. Bour, S. W. Corzine, M. R. T. Tan, and L. J. Mawst, IEEE J. Quantum Electron. **38**, 640 (2002).
[23] P. M. Smowton and P. Blood, IEEE J. Sel. Top. Quantum Electron. **3**, 491 (1997).

Downloaded 20 Jul 2011 to 128.180.137.141. Redistribution subject to AIP license or copyright; see http://apl.aip.org/about/rights_and_permissions